Now,

$$U_x(x,z) \approx U_{0_{x'}}(x',z) + 0(\epsilon) \tag{8}$$

and hence

$$U(x',z) \sim U(x,z) - \epsilon\delta x_s x_1(x')\, U_{0_x}(x',z) \tag{9}$$

Substitution of Eq. (1) into Eq. (9) gives

$$U(x',z) = U_0(x',z) + \epsilon\left[U_1(x',z) - \delta x_s\left(x_1(x')\, U_0\right)_{x'}\right] \tag{10}$$

This equation is valid in the continuous regions of the flow during the perturbation and should be independent of the straining function.

Equations (3) and (4) can be differentiated with respect to x' to give

$$U_{0_{x'x'}} + U_{0_{zz}} = \left(U_0 U_{0_{x'}}\right)_{x'} \tag{11}$$

and

$$U_{0_z}(x', \pm 0) = \pm z_{0_{x'x'}}(x') \tag{12}$$

Equation (11) can be multiplied by the function $\delta x_s x_1(x')$ and rearranged to give

$$\bar{U}_{0_{x'x'}} + \bar{U}_{0_{zz}} = \left(\bar{U}_{0_{x'}}\phi_{0_{x'}}\right)_{x'} + \delta x_s\left[x_{1_{x'}}\left(\phi_{0_{x'}} - \phi^2_{0_x}\right)\right]_{x'}$$
$$+ \delta x_s x_{1_{x'}}\left[\phi_{0_{x'}} - \tfrac{1}{2}\phi^2_{0_{x'}}\right]_{x'} \tag{13}$$

with the boundary condition

$$\bar{U}_{0_z}(x', \pm 0) = \pm\delta x_s x_1(x')\, z_{0_{x'x'}}(x') \tag{14}$$

where

$$\bar{U}_0(x',z) = \delta x_s x_1(x')\, U_0(x',z) \tag{15}$$

Now, Eq. (13) is identical with the linear Eq. (5) except that ϕ_1 is replaced by $\bar{U}_0$. Consequently, subtraction of these equations gives

$$\hat{U}_{0_{x'x'}} + \hat{U}_{0_{zz}} = \left(\hat{U}_{0_{x'}}\phi_{0_{x'}}\right)_{x'} \tag{16}$$

where

$$\hat{U}_0(x',z) = \phi_1(x',z) - \bar{U}_0(x',z) \tag{17}$$

The boundary condition is obtained from Eqs. (6) and (14). Thus,

$$\hat{U}_{0_z}(x', \pm 0) = \pm z_{1_{x'}}(x') \tag{18}$$

The problem uniquely defined by Eqs. (16) and (18) does not contain the straining function $x_1(x')$, and hence the solution $\bar{U}_0(x',z)$ is independent of the straining function.

Now, Eq. (10) can be rewritten as

$$U(x',z) = U_0(x',z) + \epsilon\hat{U}_{0_{x'}}(x',z) \tag{19}$$

Since neither $U_0(x',z)$ nor $\hat{U}_{0_{x'}}(x',z)$ are dependent on the straining function, it follows that the final velocity $U(x',z)$ is not dependent on the straining function.

Although Eqs. (17) and (18) can be solved without knowing the straining function, the usual formulation must be solved to give the physical coordinate x.

Acknowledgments

This work was sponsored by the Air Force Office of Scientific Research under Contract F49620-79-C-0054.

References

[1] Van Dyke, M., *Perturbation Methods in Fluid Mechanics,* annotated ed., Parabolic Press, Stanford, Calif., 1975.

[2] Lighthill, M.J., "A Technique for Rendering Approximate Solutions to Physical Problems Uniformly Valid," *Philosophical Magazine,* Vol. 40, No. 7, 1949, pp. 1179-1201.

[3] Nixon, D., "Perturbation of a Discontinuous Transonic Flow," *AIAA Journal,* Vol. 16, Jan. 1978, pp. 47-52.

[4] Nixon, D. "Perturbations in Two- and Three-Dimensional Transonic Flows," *AIAA Journal,* Vol. 16, July 1978, pp. 699-709.

Visualization of Flow Instabilities on a Rotating Disk

Mark H. Clarkson*
University of Florida, Gainesville, Fla.
Stanley C. Chin†
Martin Marietta Aerospace, Orlando, Fla.
and
Phillip Shacter‡
McDonnell Aircraft Company, St. Louis, Mo.

Nomenclature

r = radial coordinate
R_c = cross-flow Reynolds number
R_{δ_1} = $1.271\sqrt{R_r}$
R_0 = reference radius of disk
R_r = Reynolds number = $r^2\omega/\nu$
V_c = maximum cross-flow velocity component due to secondary flow in the boundary layer (perpendicular to flow outside boundary layer)
α = nondimensional wave number
δ_1 = boundary-layer displacement thickness for the disk = $1.271\sqrt{\nu/\omega}$
ϵ = angle between the normal to the vortex axis and the radius of the disk (see Fig. 1)
λ_α = vortex spacing measured normal to vortex axis
$\bar{\lambda}_\alpha$ = λ_α/δ_1
λ_s = wavelength of secondary instabilities
λ_ϕ = vortex spacing measured in circumferential direction at a given r
ν = kinematic viscosity
ϕ = polar coordinate angle

Background

FLOW instabilities on a rotating disk have been investigated experimentally in air by Smith,[1] who used a hot-wire probe, and by Gregory et al.,[2] who used probes and also the china clay technique. Experiments were conducted in

Presented as Paper 80-0279 at the AIAA 18th Aerospace Sciences Meeting, Pasadena, Calif., Jan. 14-16, 1980; submitted Jan. 16, 1980; revision received June 6, 1980. This paper is declared a work of the U. S. Government and therefore is in the public domain.

Index category: Boundary-Layer Stability and Transition.

*Professor, Dept. of Engineering Sciences. Associate Fellow AIAA.

†Engineer, Aerodynamics Dept. of the Systems Laboratory. Member AIAA.

‡Design Engineer, Engineering Technology Division. Member AIAA.

water by Faller and Kaylor[3] using dye and by Chin and Litt[4,5] using electrochemical probes. Among the various theoretical studies of the flow instability are those of Gregory et al.,[2] Brown,[6] and Tobak.[7] This Note deals with flow visualization of instabilities on a rotating disk in water using dye.

Description of Experiment

A 60-cm-diam clear plexiglas disk was mounted on a vertical shaft and after introduction of a cloud of sodium fluorescein dye near the lower surface, the disk was quickly rotated to a speed of about 50 rpm in a counterclockwise direction as viewed from above. Photographs were then taken from above looking through the disk. A transparent box was floated on top of the water to eliminate surface waves. Concentric circles with 25.4 mm spacing and radial lines every 15 deg were inscribed on the upper surface of the disk. The 16 mm motion pictures were taken with color film, ASA 400 rating, at 300 frames/s. An f2 zoom lens, 18-90 mm focal length, was used for most of the shots along with very short tube extensions.

A 16 mm intermittent pin-registered camera with a framing rate accuracy of ± 1% was used. Time events were measured by counting frames. Light was supplied by four 1000 W quartz iodine floodlights placed about 0.3 m (1 ft) from the walls of the tank. Insufficient light prevented higher framing rates.

Results

What one sees in dye flow visualization depends not only on the flow but also on the distribution or placement of the dye. Subsequent to the dye experiments, the technique used by Cantwell et al.[8] to study turbulent spots was utilized on the rotating disk. In these experiments, fine aluminum powder was suspended in water (1 part aluminum powder to 300 parts water by weight), and the disk was partially submerged leaving the upper surface above water. Pictures were taken, as before, through the upper surface and normal to the disk. This work is still going on, but so far agreement with the dye experiments has been close.

The following observations were made from the dye experiments. The axes of the vortices were fixed with respect to the disk and the flow spiraled around these axes downstream with respect to the disk as shown schematically in Fig. 1. As the flow spirals around the core or axis, it traps the dye and concentrates it to show the typical pattern (Fig. 2). The axes of the vortices were found to be, approximately, equiangular logarithmic spirals given by

$$r/R_0 = e^{-\phi \tan\epsilon}$$

Measurements of the dye fronts indicate that the flow is spiraling backward around the vortex core with an average velocity component along the axis of about 60-70% of ωr (measured with respect to the disk). These values correspond rather closely to a point of inflexion in the laminar boundary-layer velocity profile taken in the near radial direction. The rotational speed of the vortex was not determined.

Secondary instabilities were also observed. The initial formation of the secondary instabilities occurred at an R_r of 350,000 and, once they formed they rapidly spread radially inward to R_r's as low as 274,000. Figure 3 illustrates their general appearance just before breakup. The angle between the secondary vortex axis and the primary vortex axis varied 30-45 deg. The velocity of the secondary vortices was roughly that measured for the dye fronts of the primaries. The occurrence of these secondary instabilities was somewhat sporadic. Their lifetime was very short, approximately 0.02 s from initial formation to breakup.

Comparison of Data

In laboratory experiments conducted on Ekman layers,[3,9] two types of instabilities have been observed and analyzed.[10,11] Greenspan[10] denoted the instability associated with an inflexional velocity profile as Class B. Faller and Kaylor[3] called this type 1. Another type of instability, involving the shear stress and Coriolis force, was denoted a Class A instability by Greenspan and a type 2 instability by Faller and Kaylor. Faller and Kaylor also studied the rotating disk by suddenly increasing the rotational speed of the tank used in Ekman flows and found both types of instabilities to exist. In addition, they observed what they called "gill" instabilities which they associated with the type 2 instability.

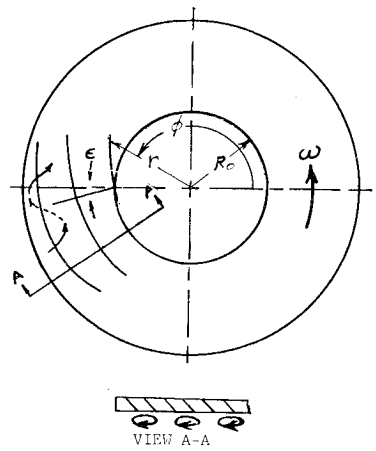

Fig. 1 Schematic of primary vortex pattern (view from above with flow observed on underside).

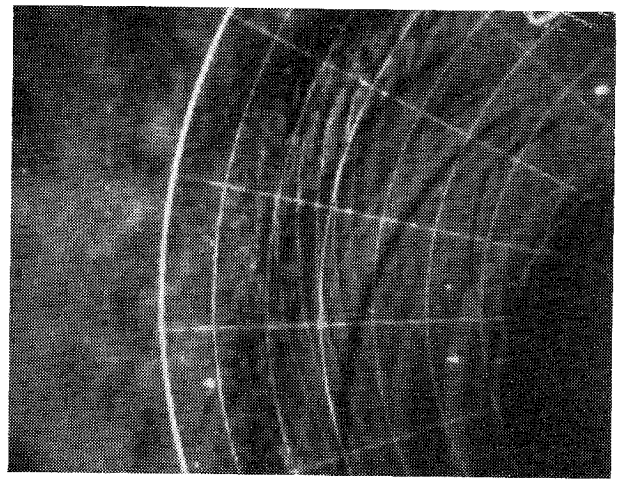

Fig. 2 $\omega = 5.07$ rad/s; primary vortices spiral outward in clockwise direction. (Note turbulent flow in outer two rings.)

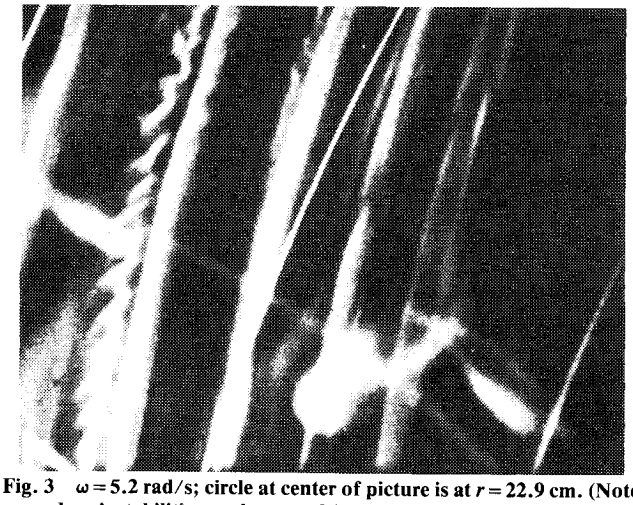

Fig. 3 $\omega = 5.2$ rad/s; circle at center of picture is at $r = 22.9$ cm. (Note secondary instabilities at about $r = 24$ cm).

Table 1 Comparison of data

Source	Onset of primary instability $\sqrt{R_r}$	$\sqrt{R_r}$ for transition to turbulence	ϵ, deg	$\bar{\lambda}_\alpha$	α	$\sqrt{R_r}$ for onset of secondary instability	$\frac{\lambda_s}{\delta_1}$
Ref. 2	427-460	520-547	14	17.5[a]	0.36	NA	NA
Ref. 3	210	400	NA	17.3	0.36	356	5.5
Ref. 4	412-480	548-592	NA	NA	NA	NA	NA
Ref. 7	–[b]	NA	11	15	0.42	NA	NA
Present work	532-621	562-680	11	15	0.42	592	6.0

NA - not available or not applicable. [a] China clay experiments. [b] Assumed range of Gregory et al.[2]

Although secondary instabilities which had characteristics similar to the "gill" instabilities were observed in our experiments, it must be concluded that they were not precisely the same thing, since in Faller and Kaylor's experiment they were associated with a type 2 instability and in our case they were associated with a type 1 instability. Type 2 instabilities were not observed in our experiments.

Owen and Randall[12] proposed a cross flow Reynolds number defined by

$$R_c = V_c \delta_1 / \nu$$

For the disk, the maximum cross-flow component is $V_c = 0.181 r\omega$ and the displacement thickness of the tangential velocity component is

$$\delta_1 = 1.271\sqrt{\nu/\omega}$$

Substitution for V_c and δ_1 yields

$$R_c = 0.230\sqrt{R_r}$$

Another Reynolds number that is used[2] is based upon the tangential velocity component and the displacement thickness which gives

$$R_{\delta_1} = r\omega\delta_1/\nu = 1.271\sqrt{R_r}$$

In either case, the pertinent parameter is $\sqrt{R_r}$.

At a given radius r, the spacing between vortices measured along the circumference of the circle is

$$\lambda_\phi = 2\pi r/N$$

where N is the number of vortices. The spacing normal to the vortex is given by

$$\lambda_\alpha = \lambda_\phi \sin\epsilon = 2\pi r \sin\epsilon / N$$

λ_α may be nondimensionalized by dividing by δ_1. This gives

$$\bar{\lambda}_\alpha = (2\pi\sin\epsilon)\sqrt{R_r}/1.271N$$

This yields a nondimensional wave number for a two-dimensional disturbance propagating in a direction normal to the vortex axes:

$$\alpha = 1.271N/(\sin\epsilon)\sqrt{R_r} = 2\pi/\bar{\lambda}_\alpha$$

A comparison of these quantities with other work is presented in Table 1.

Conclusions

By referring to Table 1, it can be seen that the appearance of the primary instability (Class B) and the transition to turbulent flow occurred at higher Reynolds numbers than those reported by other investigators.

Tobak[7] carried out numerical solutions of the Orr-Summerfeld equations for the rotating disk boundary-layer profiles and found that the stationary disturbance with the largest growth rate corresponds to a wave number of 0.4 and ϵ of 11 deg. These values agree with the present work.

It is believed that the present results should be useful for further comparisons with theory since the tank was large compared to the disk and the initial turbulence level was quite low, particularly when compared with a disk rotating in air in a room.

Acknowledgment

This work was sponsored by NASA Ames Research Center under Grant NSG-2120.

References

[1] Smith, N. H., "Exploratory Investigation of Laminar Boundary Layer Oscillations on a Rotating Disk," NACA TN 1227,1947.

[2] Gregory, N., Stuart, J. T., and Walker, W. E., "On the Stability of Three-Dimensional Boundary Layers with Applications to the Flow Due to a Rotating Disk," *Philosophical Transactions of the Royal Society of London,* Series A, Vol. 248, No. 943, July 1955, pp. 155-199.

[3] Faller, A. J. and Kaylor, R. E., "Investigations of Stability and Transition in Rotating Boundary Layers," *Dynamics of Fluids and Plasmas,* edited by S. I. Pai, Academic Press, New York, 1966, pp. 309-329.

[4] Chin, D. T. and Litt, M., "Mass Transfer to Point Electrodes on the Surface of a Rotating Disk," *Journal of the Electrochemical Society,* Vol. 119, Oct. 1972, pp. 1338-1343.

[5] Chin, D. T. and Litt, M., "An Electrochemical Study of Flow Instability on a Rotating Disk," *Journal of Fluid Mechanics,* Vol. 54, Pt. 4, 1972, pp.613-625.

[6] Brown, W. B., "Numerical Calculation of the Stability of Cross-Flow Profiles in Laminar Boundary Layers on a Rotating Disc and on a Swept-Back Wing and an Exact Calculation of the Stability of the Blasius Velocity Profile," Northrop Aircraft Rept. NAI-59-5, Jan 1959.

[7] Tobak, M., "On Local Inflexional Instability in Boundary-Layer Flows," *Zeitschrift für angewandte Mathematik and Physik,* Vol. 24, 1973, pp. 330-354.

[8] Cantwell, B., Coles, D., and Dimotakis, P., "Structure and Entrainment in the Plane of Symmetry of a Turbulent Spot," *Journal of Fluid Mechanics,* Vol. 87, Pt. 4, 1978, pp. 641-672.

[9] Tatro, P. R. and Mollo-Christensen, E. L., "Experiments on Ekman Layer Instability," *Journal of Fluid Mechanics,* Vol. 28, Pt. 3, April 1967, pp. 531-543.

[10] Greenspan, H. P., *The Theory of Rotating Fluids,* Cambridge University Press, Cambridge, England, 1968.

[11] Iooss, G., Nielsen, H. B., and Nielsen, H. T., "Bifurcation of the Stationary Ekman Flow into a Stable Periodic Flow," *Archives of Rational Mechanics and Analysis,* Vol. 68, No. 3, 1978, pp. 227-256.

[12] Owen, P. R. and Randall, D. G., "Boundary Layer Transition on a Swept Back Wing," Royal Aircraft Establishment TM Aero. 277, May 1952.